Analyst

PAPER

Cite this: *Analyst*, 2014, **139**, 5014

Highly sensitive electrochemical sensor using a MWCNTs/GNPs-modified electrode for lead (II) detection based on Pb^{2+}-induced G-rich DNA conformation

Yuan Zhu,[ab] Guang-ming Zeng,*[ab] Yi Zhang,*[ab] Lin Tang,[ab] Jun Chen,[ab] Min Cheng,[ab] Li-hua Zhang,[ab] Ling He,[ab] Yuan Guo,[ab] Xiao-xiao He,[ab] Ming-yong Lai[ab] and Yi-bin He[ab]

Received 14th May 2014
Accepted 27th June 2014

DOI: 10.1039/c4an00874j

www.rsc.org/analyst

A sensitive electrochemical lead ion (Pb^{2+}) sensor based on carboxylic acid group functionalized multi-walled carbon nanotubes (MWNTs-COOH) and direct electrodeposited gold nanoparticles (GNPs) was developed for Pb^{2+} detection. The DNA capture probe was self-assembled onto the surface of the modified electrode for hybridizing with the guanine-rich (G-rich) aptamer probe and for forming the DNA double helix structure. When Pb^{2+} was added in, the DNA duplex unwound and formed a stabilized G-quadruplex (G4) due to the Pb^{2+}-induced G-rich DNA conformation. Also, methylene blue (MB) was selected as the G4-binding indicator. Compared with previous Pb^{2+} sensors, the proposed sensor had better sensitivity, because the modified MWCNTs/GNPs could provide a large surface area and good charge-transport capacity to dramatically improve the DNA attachment quantity and sensor performance. The sensor could detect Pb^{2+} in a range from 5.0×10^{-11} to 1.0×10^{-14} M, with a detection of 4.3×10^{-15} M.

Introduction

Heavy metals contamination constitutes a severe threat to human health and the environment. In particular, lead (Pb^{2+}) causes various neurotoxin effects, including anemia, memory loss, irritability, and mental retardation, especially in children.[1–3] Therefore, an accurate, sensitive, and on-site monitoring of Pb^{2+} seems to be critical for environmental and food tracking, as well as for clinical toxicology.[4]

Electrochemical sensors have received increasing attention in recent years, because of their fast response time, remarkably high sensitivity, good selectivity, and strong operability.[5,6] In contrast to many existing techniques for lead (Pb^{2+}) detection, such as surface plasmon resonance spectroscopy (SPR),[7] quartz crystal microbalance (QCM),[8] and fluorescence,[9,10] electrochemical sensors afford a lot of advantages, such as its simplicity of use, rapidity, low cost, and high sensitivity.[11] In the present study, we developed an electrochemical sensor based on a Pb^{2+}-induced G-rich DNA conformation to detect Pb^{2+}.

In order to develop highly sensitive electrochemical sensors, many nanomaterials have been used for the modification of substrates to increase the amount of DNA immobilized at the probes and to improve the recognition capacity toward the target.[12–14] The introduction of nanomaterials can efficiently increase the electrode surface area and increase the amount of immobilized DNA. Furthermore, the nanostructure can play an important role in the orientation and assembly density, controlling the probe DNA for the optimized hybridization recognition ability.[15,16] DNA, modified with –SH, can link GNPs directly, which avoids the conductivity and reaction efficiency reducing when the electrode is modified with excessive materials and functional groups. Additionally, because GNPs have high electrical conductivity, an abundant effective surface area, and can retain high bioactivity, they are seen as beneficial for applications in sensor strategies. GNPs can be easily prepared by several different processes, including direct electrostatic assembly, polymer entrapment or co-mixing, covalent linking, sol–gel, and electro-deposition methods.[17] The electro-deposition method is one of the most widely used strategies as it offers the advantages of convenience and wide application in electrocatalysis and electroanalysis.[18,19]

Carbon nanotubes (CNTs) have a large specific surface area, surface atoms, good electrical conductivity and can reduce oxidation and reduction potential. There are several functional groups on the port and side walls of CNTs that can react with the carboxylic acid group, such as –OH, –CHO, –COOH.[20–23] In

[a]*College of Environmental Science and Engineering, Hunan University, Changsha 410082, China. E-mail: zgming@hnu.edu.cn; zyi@hnu.edu.cn; Fax: +86-731-88823701; Tel: +86-731-88822754*

[b]*Key Laboratory of Environmental Biology and Pollution Control (Hunan University), Ministry of Education, Changsha 410082, China*

this work, multi-walled carbon nanotubes (MWCNTs) were used for sensor fabrication. When MWCNTs are treated with acid, the ends and surfaces of the carbon nanotubes become covered with oxygen-containing groups, such as carboxyl and ether groups.[24,25] The modified MWCNTs can be used for improving the performance of the glassy carbon electrode (GCE). Also, GNPs were coated onto the MWCNTs-modified GCE in direct electrodeposition.[26]

With increased research into the interactions between DNA and metal ions, functional DNA molecules have become a powerful tool for Pb^{2+} detection.[27] Three DNA probes had been reported for their particular binding affinity with Pb^{2+}.[28] They are a Pb^{2+}-dependent RNA-cleaving DNAzyme called "8–17", which finds widespread use in Pb^{2+} sensors;[29] GR-5 DNAzyme;[30] and Pb^{2+}-induced allosteric G-quadruplex (G4) oligonucleotide.[31] G4s have a special higher-order structure, in which G-rich nucleic acid sequences are shaped by the stacked arrays of G-quartets, connected by Hoogsteen-type base pairing. They can react with metal ions, such as K^+, Ag^+, Hg^{2+}, Pb^{2+} *etc.* Pb^{2+}-induced G4 has the highest stability compared with other metal ions, because of the smaller diameter of Pb^{2+}.[32] Herein, we developed an electrochemical sensor based on the G4 structure of the Pb^{2+}-induced G-rich DNA conformation and the G4-binding indicator (methylene blue, MB). The DNA sensor with the T30695 molecule, 5′-$(GGGT)_4$-3′, is specific to Pb^{2+}.[33] The DNA device functions by binding Pb^{2+} to the G4 structure.[27] Pb^{2+} has been proven to have outstanding efficiency for stabilizing G4 DNA. Due to this unique feature, Pb^{2+} can damage a DNA duplex and form G4 DNA. The ultrahigh G4-stabilizing efficiency of Pb^{2+} enables the DNA device to have a high sensitivity and selectivity for sensing Pb^{2+}.

This study has assessed the characteristics of MWCNTs and GNPs and enabled us to construct a highly sensitive electrochemical sensor for Pb^{2+} detection. Pb^{2+} could induce the DNA duplex transformed into Pb^{2+}-stabilized G4.[34] As an indicator, MB released from the electrode surface, led to a clear reduction of the electric signal. Compared with the common Pb^{2+} sensor, the proposed sensor has a lower detection limit and higher sensitivity, due to the strong electronic conductivity of the modified nanomaterials and the high sensitivity of the Pb^{2+}-induced allosteric G4 oligonucleotide. The conformation of the proposed sensor had good repeatability and stable performance.

Experimental

Apparatus

Electrochemical measurements were carried out on a CHI760B electrochemistry system (Chenhua Instrument, Shanghai, China). The three-electrode system used in this work consists of a glassy carbon electrode (5 mm in diameter) as the working electrode, a saturated calomel electrode (SCE) as the reference electrode and a Pt foil auxiliary electrode. Scanning electron micrographs (SEM) of the morphology of the GCE surface were obtained with a S-4800 scanning electron microscope (Hitachi Ltd., Japan).

Reagents

MWCNTs were supplied by Applied Nanotechnologies, Inc. (Shanghai, China). Hydrochloroauric acid ($HAuCl_4 \cdot 4H_20$) was from Sinopharm Chemical Reagent Co., Ltd. (Shanghai, China). 6-Mercaptohexanol (MCH), *N*,*N*-dimethylformamide (DMF) and tris(hydroxymethyl)aminomethane (Tris) were purchased from Sigma-Aldrich (St. Louis, MO, USA). All other chemicals were of analytical grade and used as received. This work used Tris–HCl buffer (10 mM Tris adjusted to pH 8.0 with 1.0 M KCl, 10 mM Tris adjusted to pH 7.4 with 1.0 M KCl). Doubly distilled water (18MΩ) was used throughout the experiments.

The DNA probes in our experiment were synthesized by Sangon (Shanghai, China). The sequences of the oligonucleotides include: 5′-CACCCACCCAC–SH-3′ (S1, capture probe), 5′-GGGTGGGTGGGTGGGT-3′ (S2, aptamer probe).

Preparation of MWCNTs

The MWCNTs were purified by ultrasonic treatment in a mixture solution of hydrogen peroxide and sulfuric acid (1 : 3, v/v) at 50 °C for 2.5 h. Afterwards, the MWCNTs were rinsed with doubly distilled water and ethanol several times, until the pH value reached neutral; then they were filtered and dried in a vacuum at 60 °C for 24 h. This procedure shortened the nanotubes and produced carboxylic acid groups, mainly on the open ends and side walls. The MWCNTs mixed with solvent DMF were ultrasonically agitated, to give a concentration of the MWCNTs suspension as 1.0 mg mL^{-1}.[35]

Preparation of MWCNTs/GNPs/DNA modified electrode

The GCE surface was smoothed with alumina powder sized 0.05 μm on the buckskin, rinsed ultrasonically into acetone and then water and then kept dry in the air. 7.0 μL MWNTs suspension was dropped onto the freshly polished GCE surface. The electrode was thoroughly washed with ethanol, and then with ultrapure water, to remove excess nanotubes until all the solvent evaporated from the surface of the GCE. Then, the modified GCE was immersed in 5 mL of $HAuCl_4$ solution (1% wt) and 200 μL perchloric acid for electrodeposition at 0.2 V in 60 s, and dried.

30 μL of the capture probe hybridization solution (S1, 1.0 μM, containing 0.1 mM TCEP, 1 mM EDTA, 10 mM Tris–HCl buffer adjusted to pH 8.0 with 1.0 M KCl) was pipetted onto the electrode surface at 4 °C for 12 h. Then it was washed with Tris–HCl buffer (10 mM, pH 7.4). 0.2 mM MCH was dropped onto the electrode surface for 30 min and then rinsed with Tris–HCl buffer (10 mM, pH 7.4).

DNA hybridization detection

The electrode surface was coated with 30 μL 1.0 μM aptamer probe solution (S2, containing 10 mM Tris–HCl buffer adjusted to pH 8.0 with 1.0 M KCl) at 37 °C for 1 h and cleaned with Tris–HCl buffer (10 mM, pH 7.4). The electrode was immersed into 0.2 mM MB in 10 mM Tris–HCl buffer (1.0 M KCl, pH 7.4) for 20 min, and then in 10 mM Tris–HCl buffer (1.0 M KCl, pH 7.4) for

10 min and washed. It was immersed in Pb^{2+} at different concentrations.

Results and discussions

Sensing mechanism

The aptamer DNA molecule combined with Pb^{2+} far greater than it did with its complementary DNA. Therefore, this suggests the double helix structure could be unwound when Pb^{2+} was added in. The MB bound on the double helix DNA was completely released from the electrode surface, and the electrical signal thus decreased due to the change in the DNA structure.[36] The sensor strategy is shown in Fig. 1, the assembling and hybridization of the DNA biosensor are based on a Pb^{2+}-induced allosteric G4 oligonucleotide and on electrochemical detection. After fabricating the MWCNTs/GNPs electrode, S1 was self-assembled on the GNPs *via* a Au–SH interaction. MCH was dropped onto the electrode surface for 30 min in order to further eliminate the non-adsorbed DNA molecules and to keep a good orientation of the DNA probe for its high recognition ability. Then, S2 was hybridized with S1 to form the DNA duplex, and then it was treated with MB. When Pb^{2+} was added in, the DNA duplex randomly changed into Pb^{2+}-stabilized G4 due to the Pb^{2+} inducing the DNA conformation.[34] The MB released into solution from the electrode surface, led the electric signal to clearly reduce. Therefore, the current signal reduces when Pb^{2+} is added.

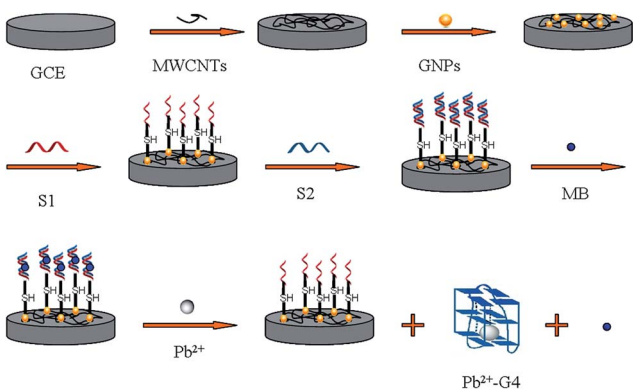

Fig. 1 Assembly and hybridization of the DNA sensor.

Electrode surface morphology

The morphology of the CPE surface was investigated by SEM. Fig. 2A shows that the MWCNTs were uniformly dispersed in DMF, and the MWCNTs pipes can be clearly seen. The pipe diameter is about 10–20 nm, and the length is up to about 10 μm. Some MWCNTs were shaped as boundless tubes because of the van der Waals forces. In Fig. 2B, MWCNTs/GNPs were evenly paved on the electrode surface to form a base layer. The high-resolution image revealed that the GNPs film was comprised of numerous spheres of about 125 nm. The spatial structure of the MWCNTs/GNPs offered many reaction sites and spaces for the hybridization process. Theoretically, the two-step procedure for the surface modification greatly improved the performance of the sensor and facilitated its practical application in electroanalysis.

Electrochemical behavior

During the modification process, electrochemical impedance spectroscopy (EIS) was applied to provide further information about the impedance change on the electrode surface. The semicircle diameter represented the electron-transfer resistance in EIS. R_{et} controlled the electron transfer kinetics of the redox probe at the electrode interface. Fig. 3A illustrated the Nyquist plot of the variously modified electrodes in a 5 mM $[Fe(CN)_6]^{3-/4-}$ phosphate buffer containing 10 mM KCl at an open circuit potential with the frequency varied from 0.01 Hz to 100 kHz. The bare GCE showed a maximum R_{et} value of about 600 Ω (curve a). With the modification of GNPs, an almost straight line was observed, implying an increase in the electron transfer ability (curve c). The R_{et} value nearly increased by 100 Ω (curve d) after being self-assembled with the DNA probe. The electron transfer ability reported by changes in the impedance of the modified electrode was in accordance with the current response reflected by the cyclic voltammetry measurements.

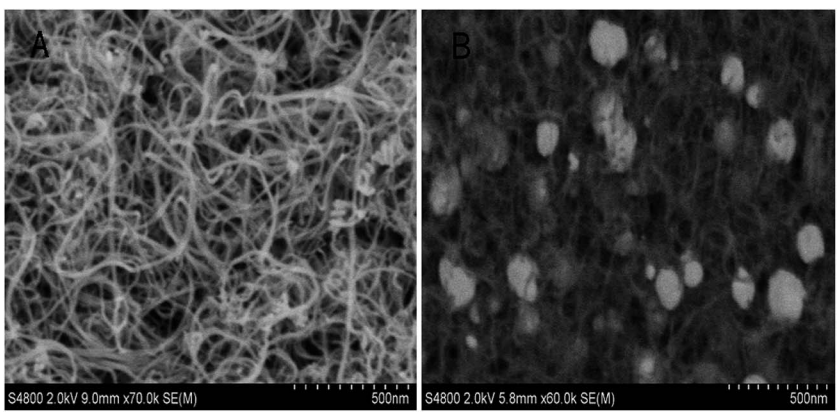

Fig. 2 Morphology of the modified electrode surface: (A) MWCNTs, (B) MWCNTs/GNPs.

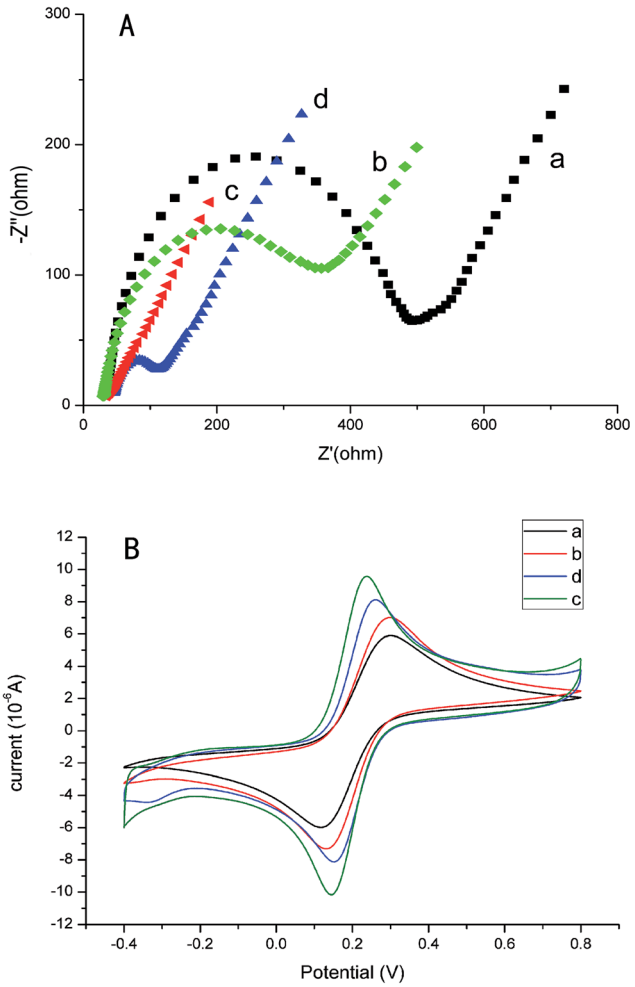

Fig. 3 Electrochemical impedance spectra (Nyquist plots) (A) of bare (a), MWCNTs (b), MWCNTs/GNPs (c), MWCNTs/GNPs/DNA (d)-modified electrode with frequency range from 0.01 Hz to 10^5 Hz; cyclic voltammograms (B) of bare (a), MWCNTs (b), MWCNTs/GNPs (c), MWCNTs/GNPs/DNA (d) modified electrode in 10 mM KCl solution containing 5.0 mM ferricyanide at a scan rate of 100 mV s^{-1}.

In Fig. 3B, cyclic voltammetry (CV) was carried out to test the property of the modified electrode. A pair of well defined redox peaks are shown on the bare GCE, with anodic and cathodic peak potentials of 0.26 V and 0.13 V, respectively (curve a). With the modification of the MWCNTs, the peak current increased (curve b). After the electro-deposition of Au, the peak current increased slightly, which indicated that there was a better redox behavior of $Fe(CN)_6^{3-}/Fe(CN)_6^{4-}$ on the MWCNTs/GNPs modified electrode (curve c). When self-assembled on the DNA probe, the peak current decreased slightly (curve d). This could be explained by the negative charge increasing the repellence of the redox species. These cyclic voltammograms proved that the modified electrode had a good current response capability.

Optimization of detection conditions

Optimization of the reaction conditions included the reaction times of MB, the reaction times of S2 and Pb^{2+}, the electrodeposition times of GNPs, and the current signals in different pH solutions. The detection method used was differential pulse voltammetry (DPV).

The reaction time of MB in the detection system was optimized based on the induced maximum current change. As shown in Fig. 4A, the MB signal on the MWCNTs/GNPs/DNA-modified electrode was rapidly enhanced with increasing the reaction time of MB. Also, the current signal of MB changed slowly after 15 min in 1.0×10^{-12} M Pb^{2+} solution. Therefore, 20 min was chosen as the optimum immobilization time.

The reaction time between S2 and Pb^{2+} had great influence on the Pb^{2+} performance. The peak current difference increased over 30 min and reached its maximum peak upon exposure to 1.0×10^{-12} M Pb^{2+} solution. Therefore, we use 30 min as the optimal reaction time between S2 and Pb^{2+} (Fig. 4B).

The time of electrodeposition GNPs was optimized in 1.0×10^{-12} M Pb^{2+} solution as shown in Fig. 4C. The current increased over 60 s and then decreased. When the electrodeposition time for GNPs was less than 60 s, the amount of DNA immobilized on the modified electrode became less, and the current signals became weaker. On the contrary, after 80 s GNPs would completely cover MWCNTs and reduce the effect of MWCNTs. Therefore, 60 s was employed as the optimum electrodeposition time for GNPs.

pH level can also affect the reaction system. Fig. 4D shows the peak current difference of the MWCNTs/GNPs/DNA-modified electrode in different pH buffer solutions. The electric signal reached the maximum when the pH was 7.4. This indicated that the double helix structure was unzipped and that the production of Pb^{2+}-stabilized G4 increased to a maximum in the same concentration of Pb^{2+} solution. Hence, pH 7.4 was noted as the best pH level to maintain the detection in good condition.

Response of the sensor to Pb^{2+} concentrations

The double helix structure was unwound and Pb^{2+} induced the DNA conformation to change into Pb^{2+}-stabilized G4 at random when the target was added. MB was completely released from the electrode surface, and the electrical signal was smaller than before the DNA double stranded form changed. Fig. 5A reflected the DPV showing that the MWCNTs/GNPs/DNA system reacted with Pb^{2+}. The DPV peak current of MB on the modified electrode increased with the declining concentration of Pb^{2+}, which ranged from 5.0×10^{-11} to 1.0×10^{-14} M with the following regression equation:

$$Y = -(7.660 \pm 0.363) - (1.035 \pm 0.03118)\chi. \quad (1)$$

In Fig. 5B, the change of the peak current linear regression coefficient result was 0.994 and for low detection was obtained as 4.3×10^{-15} M ($S/N = 3$). Table 1 shows that the sensitivity of the electrochemical DNA sensor is superior to other current DNAzyme-based biosensors for detecting Pb^{2+} using fluorescence, electrochemiluminescence (ECL), and electrochemical

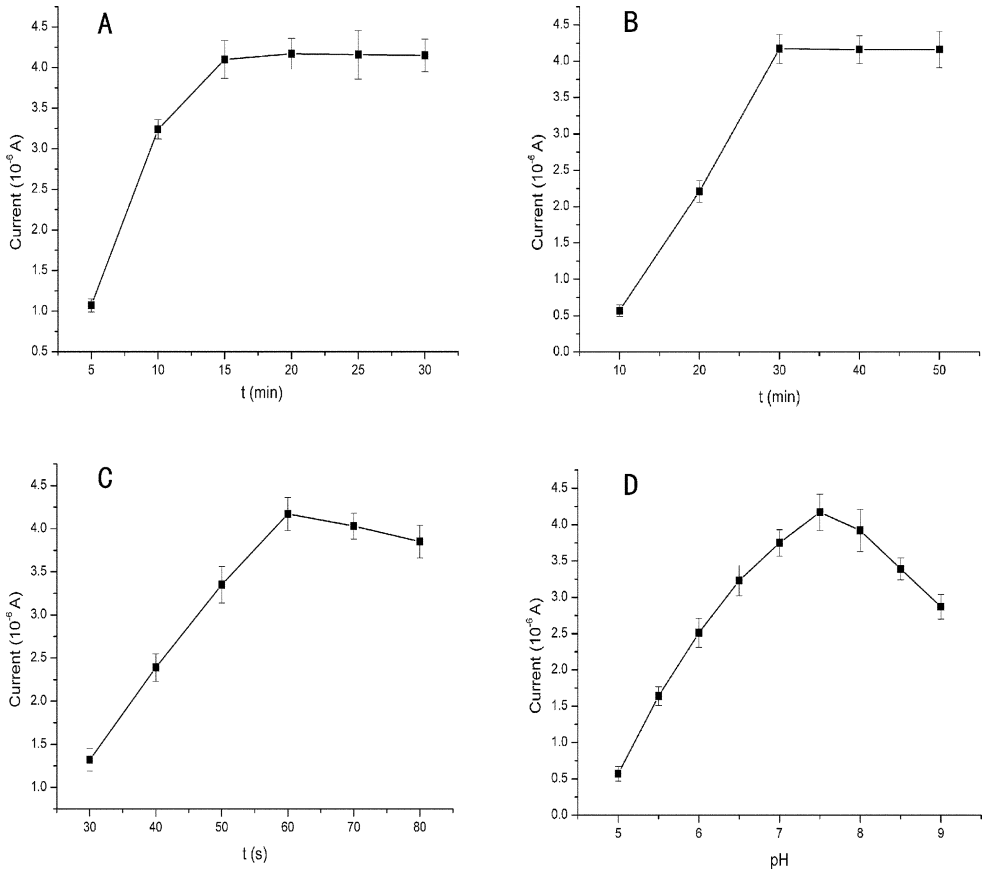

Fig. 4 The MB current signals on the modified electrode at different MB reaction times (A); S2 and Pb^{2+} reaction times (B); electrodeposition GNPs times (C); the current signals in different pH solution (D).

methods.[27,37–49] The developed sensors could completely meet the requirement of water quality monitoring.

Repeatability, reusability and selectivity

Repeatability studies were carried out by successive measurements ($N = 10$) using the same sensor in a concentration of 1.0×10^{-12} M Pb^{2+} solution under the same above-mentioned procedures and conditions. The experimental results revealed that the Relative Standard Deviations (RSD) was 4.9%. The repeatability was also carried out with five different GCEs constructed by the same steps but independently. RSD was 4.8%, indicating that the fabrication procedure was reliable and that the modified GCE had a good repeatability.

The reusability was investigated as follows: the electrode was treated in Piranha solution (mixture of H_2SO_4 and H_2O_2 with a volume ratio of 3 : 2) at 60 °C for 30 minutes, to reach the initial state, with the removal of organic matter on its surface. Then the capture probes could be self-assembled again on the electrode for reuse. This could last for 3 cycles, where 78% of the original current response was observed.

In order to investigate the selectivity of the electrochemical sensor for Pb^{2+} detection, several potential interference metal ions were tested, such as Ca^{2+}, Mg^{2+}, Zn^{2+}, Fe^{3+}, Cd^{2+}, Al^{3+}, Ni^{2+}, Cu^{2+}, Mn^{2+}, K^+, Ag^+, and Hg^{2+}. As shown in Fig. 6, all the ions (1.0×10^{-12} M) except Pb^{2+} exhibited little current changes. It is clear that the largest current increase was induced by Pb^{2+}, and $Hg^{2+}$and Ag^+ had little impact. They may react with T and multiple G residues that the probe DNA molecules contained and change their random conformation.[50,51] K^+ is efficient for the stabilization of the probe DNA,[34] but it is less compact with Pb^{2+}-stabilized G4.[52] Therefore, Pb^{2+} produced the most current changes, and this electrochemical sensor had good selectivity for Pb^{2+}.

Analysis of environmental samples

In order to demonstrate the application of the proposed method, a known concentration of Pb^{2+} was spiked in tap water, water from the Xiangjiang River, and in spring water from Yuelu Mountain. All the samples were filtered through a 0.2 μm membrane before the detection measurements were performed. The tap water sample was collected after discharging tap water for about 30 min and boiling for 10 min to remove chlorine, then its pH was adjusted to 7.4 with Tris–HCl buffer. The results are shown in Table 2. The average recoveries ranged from 100.1% to 96.2% over three measurements, suggesting good accuracy of the proposed method for Pb^{2+} detection in the samples.

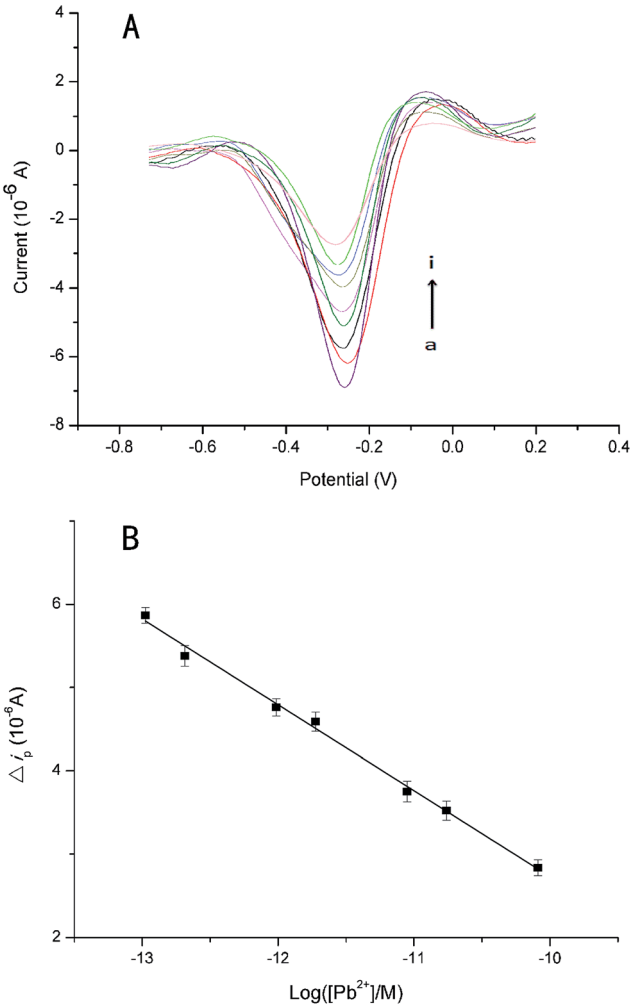

Fig. 5 DPV responses of MB for Pb^{2+} detection (A). Concentration of Pb^{2+}: 0 M (a), 1.0×10^{-14} M (b), 5.0×10^{-14} M (c), 1.0×10^{-13} M (d), 5.0×10^{-13} M (e), 1.0×10^{-12} M (f), 5.0×10^{-12} M (g), 1×10^{-11} M (h), and 5.0×10^{-11} M (i). The linear relationship between the DPV peak current change and the logarithm of the concentrations of Pb^{2+} (B).

Table 1 Comparison of the detection methods of Pb^{2+}

Target	Detection limit	Detection method	Ref.
Pb^{2+}	8.3×10^{-7} M	Electrochemical detection	37
	1.0×10^{-8} M	Fluorescence detection	38
	2.0×10^{-8} M	Electrochemical detection	39
	6.0×10^{-8} M	Fluorescence detection	40
	3.7×10^{-9} M	Fluorescence detection	41
	4.0×10^{-9} M	Electrochemical detection	42
	5.0×10^{-9} M	Fluorescence detection	27
	1.28×10^{-10} M	Fluorescence anisotropy	43
	2.0×10^{-10} M	Electrochemical detection	44
	4.0×10^{-10} M	Fluorescence anisotropy	45
	2.8×10^{-11} M	Electrochemical detection	46
	5.0×10^{-12} M	Electrochemiluminescence	47
	6.4×10^{-12} M	Electrochemical detection	48
	1.0×10^{-19} M	Electrochemical detection	49
	4.3×10^{-15} M	Electrochemical detection	This work

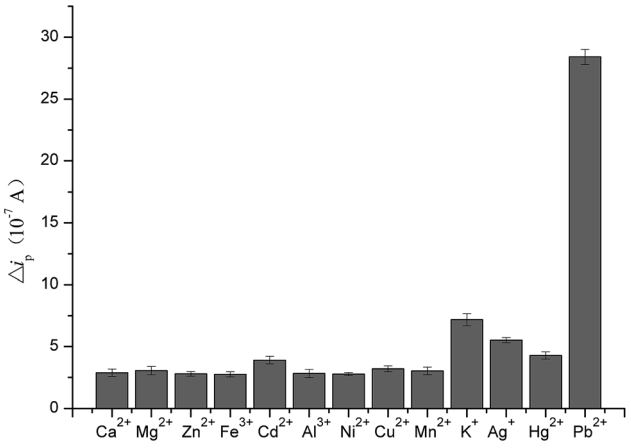

Fig. 6 Selectivity of the electrochemical sensor for Pb^{2+}. The concentration of Pb^{2+} and other metal ions were kept at 1.0×10^{-12} M.

Table 2 Determination of Pb^{2+} in water sample

Sample	Added (10^{-12} M)	Result (10^{-12} M)	Recovery (%)
Tap water	10	9.62 ± 0.29	96.2
Spring water	50	49.85 ± 0.17	99.7
River water	100	100.13 ± 0.34	100.1

Conclusion

An electrochemical strategy was developed for the highly sensitive and selective detection of Pb^{2+} using a MWCNTs/GNPs/DNA-modified electrode. The sensor showed a very low electron transfer resistance, due to the presence of MWCNTs and GNPs, which greatly improved the sensitivity of detection. The structure of GNPs assembled on the MWCNTs-modified GCE was favorable for combining with DNA, whereby the double helix structure was unwound and Pb^{2+}-stabilized G4 was formed when Pb^{2+} was added. MB was released into solution, and the electrical signal diminished before the DNA structure changed. The optimized DNA biosensor could achieve a wide linear range from 5.0×10^{-11} to 1.0×10^{-14} M for Pb^{2+} detection, with a low detection limit of 4.3×10^{-15} M. The sensor showed good selectivity and could determine Pb^{2+} in natural water samples with satisfactory results, and thus offers a potential application in the on-site monitoring of lead pollution samples in the environment.

Acknowledgements

This study was financially supported by the National Natural Science Foundation of China (51039001, 51378190), the fundamental Research Funds for the Central Universities, Hunan University, the Top Young Talents Program from Chinese Government, the Program for Changjiang Scholars and Innovative Research Team in University (IRT-13R17) and the

Hunan Provincial Innovation Foundation For Postgraduate (CX2009B080).

References

1 D. Bellinger, A. Leviton, J. Sloman, M. Rabinowitz, H. L. Needleman and C. Waternaux, *Pediatrics*, 1991, **87**, 219–227.
2 G. M. Zeng, M. Chen and Z. T. Zeng, *Science*, 2013, **340**, 1403.
3 G. M. Zeng, M. Chen and Z. T. Zeng, *Nature*, 2013, **499**, 154.
4 T. Sokalski, A. Ceresa, T. Zwickl and E. Pretsch, *J. Am. Chem. Soc.*, 1997, **119**, 11347–11348.
5 Y. Zhang, G. M. Zeng, L. Tang, Y. P. Li, L. J. Chen, Y. Pang, L. Zhen, C. L. Feng and G. H. Huang, *Analyst*, 2011, **136**, 4204–4210.
6 J. P. Xie, Y. G. Zheng and J. Y. Ying, *Chem. Commun.*, 2010, **46**, 961–963.
7 N. Matsuura, D. J. Elliot, D. N. Furlong and F. Grieser, *Colloids Surf., A*, 1997, **126**, 189–195.
8 C. Ayela, F. Roquet, L. Valera, C. Granier, L. Nicu and M. Pugniere, *Biosens. Bioelectron.*, 2007, **22**, 3113–3119.
9 Z. Li, C. G. Niu, G. M. Zeng, Y. Liu, P. Gao, G. H. Huang and Y. Mao, *Sens. Actuators, B*, 2006, **114**, 308–315.
10 Y. Zhang, G. M. Zeng, L. Tang, C. Liu, Y. Pang, L. J. Chen, C. L. Feng and G. H. Huang, *Talanta*, 2010, **83**, 210–215.
11 A. A. Lubin, B. V. S. Hunt, R. J. White and K. W. Plaxco, *Anal. Chem.*, 2009, **81**, 2150–2158.
12 Y. Zhang, G. M. Zeng, L. Tang, D. L. Huang, X. Jiang and Y. Chen, *Biosens. Bioelectron.*, 2007, **22**, 2121–2126.
13 Y. Zhang, G. M. Zeng, L. Tang, Y. P. Li, Z. Chen and G. Huang, *RSC Adv.*, 2014, **4**, 18485–18492.
14 F. Xia, X. Zuo, R. Yang, Y. Xiao, D. Kang, A. Vallee-Belisle, X. Gong, J. D. Yuen, B. B. Y. Hsu, A. J. Heeger and K. W. Plaxco, *Proc. Natl. Acad. Sci. U. S. A.*, 2010, **107**, 10837–10841.
15 J. Hahm and C. M. Lieber, *Nano Lett.*, 2004, **4**, 51–54.
16 H. Sun, T. S. Choy, D. R. Zhu, W. C. Yam and Y. S. Fung, *Biosens. Bioelectron.*, 2009, **24**, 1405–1410.
17 I. Willner, B. Shlyahovsky, M. Zayats and B. Willner, *Chem. Soc. Rev.*, 2008, **37**, 1153–1165.
18 L. Wang, W. Mao, D. Ni, J. Di, Y. Wu and Y. Tu, *Electrochem. Commun.*, 2008, **10**, 673–676.
19 J. Deng, Y. Song, Y. Wang and J. Di, *Biosens. Bioelectron.*, 2010, **26**, 615–619.
20 M. W. Marshall, S. Popa-Nita and J. G. Shapter, *Carbon*, 2006, **44**, 1137–1141.
21 P. Xu, G. M. Zeng, D. L. Huang, C. L. Feng, S. Hu, M. H. Zhao, C. Lai, Z. Wei, C. Huang, G. X. Xie and Z. F. Liu, *Sci. Total Environ.*, 2012, **424**, 1–10.
22 W. W. Tang, G. M. Zeng, J. L. Gong, J. Liang, P. Xu, C. Zhang and B. B. Huang, *Sci. Total Environ.*, 2014, **468–469**, 1014–1027.
23 J. L. Gong, B. Wang, G. M. Zeng, C. P. Yang, C. G. Niu, Q. Y. Niu, W. J. Zhou and Y. Liang, *J. Hazard. Mater.*, 2009, **164**, 1517–1522.
24 S. Wang and Q. Xu, *Bioelectrochemistry*, 2007, **70**, 296–300.
25 G. J. Hua, J. B. Li and G. M. Zeng, *J. Hazard. Mater.*, 2013, **261**, 470–490.
26 N. Alexeyeva and K. Tammeveski, *Anal. Chim. Acta*, 2008, **618**, 140–146.
27 T. Li, S. Dong and E. K. Wang, *J. Am. Chem. Soc.*, 2010, **132**, 13156–13157.
28 R. Freeman, X. Liu and I. Willner, *J. Am. Chem. Soc.*, 2011, **133**, 11597–11604.
29 T. H. M. Kjällman, H. Peng, C. Soeller and J. Travas-Sejdic, *Anal. Chem.*, 2008, **80**, 9460–9466.
30 X. H. Zhao, R. M. Kong, X. B. Zhang, H. M. Meng, W. N. Liu, W. H. Tan, G. L. Shen and R. Q. Yu, *Anal. Chem.*, 2011, **83**, 5062–5066.
31 B. Yin, B. Ye, W. Tan, H. Wang and C. Xie, *J. Am. Chem. Soc.*, 2009, **131**, 14624–14625.
32 L. Guo, D. Nie, C. Qiu, Q. Zheng, H. Wu, P. Ye and Y. Hao, *Biosens. Bioelectron.*, 2012, **35**, 123–127.
33 T. Liedl and F. C. Simmel, *Nano Lett.*, 2005, **5**, 1894–1898.
34 I. Smirnov and R. H. Shafer, *J. Mol. Biol.*, 2000, **296**, 1–5.
35 T. Takenobu, T. Takano, M. Shiraishi, Y. Murakami, M. Ata, H. Kataura, Y. Achiba and Y. Iwasa, *Nat. Mater.*, 2003, **2**, 683–688.
36 J. Yoshizumi, S. Kumamoto, M. Nakamura and K. Yamana, *Analyst*, 2008, **133**, 323–325.
37 L. C. S. Figueiredo-Filho, B. C. Janeqitz, O. Figueiredo-Filho, L. H. Marcolino-Junior and C. E. Banks, *Anal. Methods*, 2013, **5**, 202–207.
38 S. Liu, W. Na, S. Pang and X. Su, *Biosens. Bioelectron.*, 2014, **58**, 17–21.
39 Z. E. Jacobi, L. Li and J. Liu, *Analyst*, 2012, **137**, 704–709.
40 X. Li, B. Xu, H. Lu, Z. Wang, J. Zhang, Y. Zhang, Y. Dong, K. Ma, S. Wen and W. Tian, *Anal. Methods*, 2013, **5**, 438–441.
41 S. Zhan, Y. Wu, L. Liu, H. Xing, L. He, X. Zhan, Y. Luo and P. Zhou, *RSC Adv.*, 2013, **3**, 16962–16966.
42 F. Li, Y. Feng, C. Zhao and B. Tang, *Chem. Commun.*, 2011, **47**, 11909–11911.
43 C. H. Chung, J. H. Kim, J. Jung and B. H. Chung, *Biosens. Bioelectron.*, 2013, **41**, 827–832.
44 W. Li, Y. Yang, J. Chen, Q. Zhang, Y. Wang, F. Wang and C. Yu, *Biosens. Bioelectron.*, 2014, **53**, 245–249.
45 X. Li, G. Wang, X. Ding, Y. Chen, Y. Guo and Y. Lu, *Phys. Chem. Chem. Phys.*, 2013, **15**, 12800–12804.
46 X. Yang, J. Xu, X. Tang, H. Liu and D. Tian, *Chem. Commun.*, 2010, **46**, 3107–3109.
47 H. Xu, P. Xu, S. Gao, S. Zhang, X. Zhao, C. Fan and X. Zuo, *Biosens. Bioelectron.*, 2013, **47**, 520–523.
48 Y. Wu, Z. Cai, G. Wu, M. Rong, Y. Jiang, C. J. Yang and X. Chen, *Sens. Actuators, B*, 2014, **191**, 60–66.
49 X. Chen, R. Tian, Q. Zhang and C. Yao, *Biosens. Bioelectron.*, 2014, **53**, 90–98.
50 S. Katz, *Nature*, 1962, **194**, 569.
51 X. H. Zhou, D. M. Kong and H. X. Shen, *Anal. Chem.*, 2009, **82**, 789–793.
52 F. W. Kotch, J. C. Fettinger and J. T. Davis, *Org. Lett.*, 2000, **2**, 3277–3280.